www.czasopisma.pan.pl PAN www.journals.pan.pl

ARCHIVES of FOUNDRY ENGINEERING

ISSN (2299-2944)
Volume 2023
Issue 3/2023

110 – 117

10.24425/afe.2023.146669

14/3

Published quarterly as the organ of the Foundry Commission of the Polish Academy of Sciences

Effect of Alloying Additives and Casting Parameters on the Microstructure and Mechanical Properties of Silicon Bronzes

D. Witasiak [a, b], A. Garbacz-Klempka [a, *], M. Papaj [b], P. Papaj [b], M. Piękoś [a], J. Kozana [a], M. Maj [a], M. Perek-Nowak [a]

[a] AGH University of Science and Technology, Faculty of Foundry Engineering, Poland

[b] Metal-Kolor Starachowice, Poland

* Corresponding author. E-mail address: agarbacz@agh.edu.pl

Received 04.07.2023; accepted in revised form 16.08.2023; available online 18.09.2023

Abstract

The studied silicon bronze (CuSi3Zn3Mn1) is characterised by good strength and corrosion resistance due to the alloying elements that are present in it (Si, Zn, Mn, Fe). This study analysed the casting process in green sand moulding, gravity die casting, and centrifugal casting with a horizontal axis of rotation. The influences of Ni and Zr alloying additives as well as the casting technology that was used were evaluated on the alloy's microstructure and mechanical properties. The results of the conducted research are presented in the form of the influence of the technology (GS, GZ, GM) and the content of the introduced alloy additives on the mechanical parameters (UTS, A10, and Proof Stress, BHN).

The analysis of the tests that were carried out made it possible to determine which of the studied casting technologies had the best mechanical properties. Microstructure of metal poured into metal mould was finer than that which was cast into moulding compound.

Mechanical properties of castings made in moulding compound were lower than those that were cast into metal moulds. Increased nickel content affected the BHN parameter.

Keywords: Innovative foundry technologies and materials, Centrifugal casting, Sand casting, Mechanical properties, Microstructure

1. Introduction

Due to its properties (especially its high electrical and thermal conductivity and corrosion resistance), copper is widely used in technology and industry [1-4]. Its good technological properties allow it to be cast and machined as well as welded, and machined copper castings can be made in both sand and metal moulds (centrifugal and pressure casting is also possible). Making castings from pure copper is technologically difficult when considering the other non-ferrous metals. The metal is characterised by low flowability, high shrinkage, and its tendency towards hot cracking [1-8].

Copper alloys have a much wider range of applications than copper in its pure form. Brasses and bronzes are most commonly used in foundries. Cast bronzes are usually multi-component, and the introduced alloying additives favourably influence their properties [9-13].

Silicon bronzes are alloys of copper with silicon as the main additive (its amount in the alloy not exceeding 5%). Due to their unsuitable alloying properties, Cu-Si double alloys have not found use as materials that are used in the casting industry. Depending on the conditions under which a given casting is to work, other elements such as zinc, manganese, iron, lead, and nickel can be introduced into Cu-Si double alloys [8].

CuSi3Zn3Mn1 bronze is characterised by good casting properties [8,14]. As an alloying component, silicon acts as a deoxidiser, which has a favourable effect on the bronze alloy; as the silicon content increases, the tensile strength and hardness also increase. Unfortunately, the alloy's elongation also decreases. In addition to silicon, the alloy's flowability is also affected by the zinc that is contained in the alloy. Thanks to its good flowability, the bronze reflects the cavity of a casting mould very well. The manganese that was contained in the alloy under study increased the corrosion resistance and had a beneficial effect on the strength.

The addition of nickel to silicon bronzes can be considered to be beneficial. In cast silicon bronzes, this affects bearing properties and strengths at higher temperatures. The bronze in question has good sliding properties, machinability, and corrosion resistance [6-9].

CuSi3Zn3FeMn1 bronze is used for heavy-duty machine parts and components that are exposed to variable loads as well as parts that operate in corrosive environments [9-15].

The production of castings in moulding sand (GS) is very popular; this technology is eagerly chosen by foundries due to its low cost, the recyclability of the raw materials [16]. Moulding sand consists of quartz sand, water, and a binder. In moulding sand technology, a liquid casting melt is poured into a mould cavity through a gating system that includes a pouring basin, a sprue, a runner, and ingates. The mould in this technology consists of a bottom part and a top part; after a casting has solidified, the mould is then broken [16,17].

Despite being widely used, moulding compound technology can cause difficulties in producing high-quality castings. The main causes of defects are an improperly selected gating system, the moisture content of the mass, the low permeability of the mould, and metal outgassing [16,18].

Gravity die casting (GM) is characterised by feeding liquid casting alloy into a metal die without external pressure, filling the mould cavity by the gravity flow of the alloy through the gating system. Metal moulds are reusable moulds and are used for mass production. Castings that are made with this technology are characterised by high dimensional accuracy and a surface quality that is better than sand mould castings. Due to the rate of heat absorption by the metal moulds, castings that are made with this technology have a fine-grained structure; this favourably affects the mechanical properties of the castings [19,20].

The quality of castings that are made by gravity into metal moulds is influenced, among other things, by the temperature of the die and the coverage of the mould cavity [21].

The process of making castings in a centrifugal machine (GZ) involves feeding liquid alloy into a metal die that rotates along one axis [22]. When the liquid metal touches the inside of the die, it begins to rotate under the action of centrifugal force. During the process, we can distinguish two stages: the gravitational stage, and the stage of the centrifugal process after contact between the metal and the die [23]. This technology is advantageous due to economic and technological aspects, among others. To the first group, we can include the reduction of technological allowances, the reduction of shortages, and the lack of waste in the form of cores. Technologically, castings that are made by centrifugal casting are characterised by very good strength parameters, uniform structures, and relatively fine structures; these all positively affect the mechanical properties of the castings [24]. The quality of the casting that is produced is determined by the speed of the die, the rate of the metal feed [24-27].

The crystallization conditions resulting from the casting mould technology used affect, among other things, the structure of castings. The structures present are characterized by different plastic deformation tendencies, which affect the mechanical properties of the castings produced. Areas of columnar structure will be characterized by different properties than zones of equiaxial structure present in the casting [28-30].

2. Methodology and conditions of research

In order to determine the effect of nickel, zirconium and the casting technology on the mechanical properties and microstructure of the bronze under study (CuSi3Zn3Mn1), a series of experimental melts were performed. The starting alloy was a standardised CuSi3Zn3Mn1 bronze with the chemical composition that is included in the PN-91/H-87026 standard. The first experimental melt (Stage 01) conformed to the standard that was quoted above, and Alloy 2 (Stage 02) contained 0.97% nickel (still within the limits of the quoted standard). In the next alloy (Stage 03), the nickel content was increased to 1.8%. In the final alloy (Stage 04) (with a nickel content of 1.8%), a modifier in the form of a CuZr10 mordant was introduced. The zirconium content in Alloy 4 was 0.2%. The chemical compositions of the melts that were carried out are summarised in Table 1.

Table 1.
Chemical compositions of experimental samples

Stage	Concentration (wt.%)							
	Cu	Zn	Pb	Mn	Fe	Ni	Si	Zr
01	89.4	4.93	0.31	0.63	0.65	0.04	3.75	0.00
02	89.1	4.53	0.29	0.60	0.60	0.97	3.69	0.00
03	88.7	4.31	0.27	0.56	0.58	1.85	3.48	0.00
04	88.6	4.23	0.27	0.54	0.56	1.82	3.51	0.20

In order to determine the effects of the casting parameters on the properties of the alloys, castings were made as follows: into a moulding compound, in a metal die, and in a centrifugal casting in a machine with a horizontal axis of rotation. The dimensions of the sleeve is shown in Fig. 1.

Classic moulding sand in production circulation was used for the technological tests. The moisture content of the mass was 2%, and the cavity of the casting mould was spray-painted with an alcohol-based coating. The mould had a temperature of about 20°C (the prevailing temperature on the production floor).

The cast-iron die for gravity casting was heated to within a temperature range of 200°–270°C. Before the pouring process, the die was spray-coated with a talc-based separator.

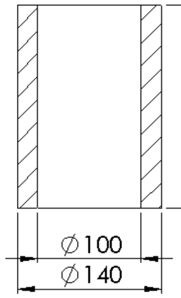

Fig. 1. Sleeve cast of silicon bronzes Ø140 x Ø100 x 200

A cast-iron die mounted in a centrifugal machine was used to make the centrifugal casting. The speed of the centrifugal machine with a horizontal axis of rotation was selected based on a nomogram, taking the optimal number of rotations into account depending on the diameter of the bushing [10,14].

The bushing was cast according to the standard parameters that are used in the centrifugal casting of silicon bronzes (990 rpm). The casting parameters of the centrifugal bushing were as follows: a pouring temperature of 1095ºC, and a die temperature of 250ºC.

The chemical composition of the cast alloys that were made for the study was analysed using a PMI-MASTER PLUS X-ray spectrometer. NIKON SMZ 745Z and Eclipse LV 150 (OM) microscopes were used to study the macro- and microstructures. Observations of the alloy were also made using a Hitachi S-3400N scanning electron microscope (SEM) with an Energy Dispersive X-ray Spectrometer (EDS) from Thermo Noran.
Strength tests were carried out on an INSTRON Model 1115.

3. Influence of alloy additions and casting parameters on metallographic properties

For macroscopic and microscopic analyses, samples were taken from castings that were made in classic moulding compounds, by gravity in a cast-iron die, and a centrifugal bushing. The sample from the centrifugal bushing was taken from the middle of the wall thickness; this was dictated by the fact that, under industrial conditions, up to 30% of the wall thickness is used as a technological allowance. The parameters of the sand castings and gravity die castings are given in Tables 2 and 3, respectively.

Table 2.
Casting parameters for sand castings (**Stages 01s–04s**)

Experiment	Metal temperature [ºC]	Sand mould temperature [ºC]
Stage 01s sand casting CuSi3Zn3Mn1	1100	20
Stage 02s sand casting CuSi3Zn3Mn1+0.9%Ni	1095	20
Stage 03s sand casting CuSi3Zn3Mn1+1.8%Ni	1100	20
Stage 04s sand casting CuSi3Zn3Mn1+1.8%Ni+0.2%Zr	1100	20

Table 3.
Casting parameters for gravity die castings (Stages **01d–04d**) and centrifugal casting (**Stage 04c**)

Experiment	Metal temperature [ºC]	Metal mould temperature [ºC]
Stage 01d gravity die casting CuSi3Zn3Mn1	1100	270
Stage 02d gravity die casting CuSi3Zn3Mn1+0.9%Ni	1095	268
Stage 03d gravity die casting CuSi3Zn3Mn1+1.8%Ni	1100	200
Stage 04d gravity die casting CuSi3Zn3Mn1+1.8%Ni+0.2%Zr	1100	250
Stage 04c centrifugal casting CuSi3Zn3Mn1+1.8%Ni+0.2%Zr	1095	250

Figures 2-4 show an image of the macrostructure of the CuSi3Zn3FeMn1 alloy. Figure 2 (sand mould casting) shows a coarse crystalline structure with an area of columnar crystals oriented from the outer surface toward the center. In the central area of the ingot, the crystals are equiaxial.

Figure 3 (gravity casting into a metal mould) there is a narrow zone of columnar crystals at the outer edge of the ingot - the effect of the metal mould during solidification - directional crystallization. Outside this zone, there are equiaxial crystals.

Figure 4 (casting of a sleeve made by the centrifugal method) Microstructure fine-grained with crystals oriented perpendicular to the axis of rotation of the mould. An arrangement of crystals similar in structure to columnar crystals can be observed. The sample was taken from a machined casting as a result of which there is no distinct zone of columnar crystals near the wall of the metal mold in the analysed surface. The uniform grain size across the casting wall guarantees stable and reproducible properties of the manufactured products.

Figures 5 and 8–10 show the microstructures of the CuSi3Zn3Mn1 bronze castings that were made in bentonite paste. Figure 5 shows the dendrites of the solid solution and the intermetallic compounds that were present at the grain boundary. The presence of iron and manganese in the alloy improved the strength properties of the alloy. The microstructures with increased nickel contents (0.9 and 1.8% Ni) are shown in Figures 8 and 9, respectively. The nickel in the alloy formed an Ni2Si compound (which was a separate component).

Figure 10 shows the microstructure of the CuSi3Zn3Mn1 bronze with 0.2% zirconium added and the nickel content increased to 1.8%. Used as a modifier, the zirconium caused the formation of wall crystals and the disappearance of the dendritic structure of the solid solution. The microstructures of the samples that were taken from the metal mould are shown in Figures 6 and 11–13. Faster heat dissipation through the material caused significant fragmentation of the microstructures. The dendrites of the solid solution of the reference sample (Figure 5) fragmented. Similar to the castings for the bentonite mass, the increased amount of nickel that was introduced into the alloy was visible as Ni2Si silicide. Introduced as a modifier, the zirconium caused the formation of wall crystals (Fig.13).

The microstructure that was taken from the casting that was made in the centrifugal machine with a horizontal axis of rotation is shown in Figure 7. We can observe how the centrifugal force affected the microstructure of the alloy under study.

As in the case of the sample that was taken from the gravity casting into the die, the microstructure showed an α solid solution and the occurrence of intermetallic phases – especially at the grain boundary.

Fig.2 . Macrostructure of CuSi3Zn3FeMn1 alloy in sand casting

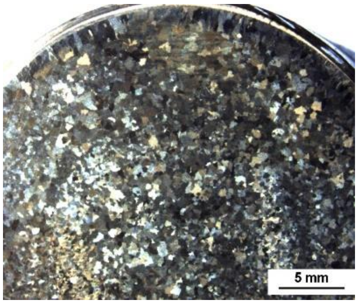

Fig.3 . Macrostructure of CuSi3Zn3FeMn1 alloy of gravity die casting

Fig. 4. Macrostructure of CuSi3Zn3FeMn1 alloy from fragment of sleeve in centrifugal casting

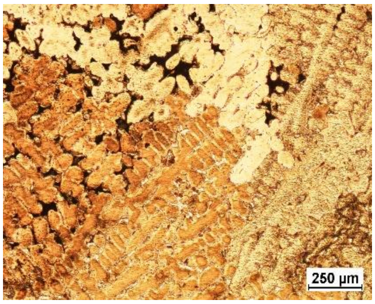

Fig. 5. Microstructure of CuSi3Zn3FeMn1 alloy in sand casting (**Stage 01s**)

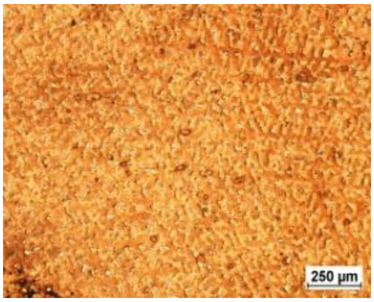

Fig. 6. Microstructure of CuSi3Zn3FeMn1 alloy of gravity die casting (**Stage 01d**)

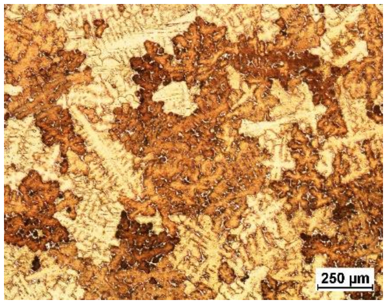

Fig. 7. Microstructure of CuSi3Zn3FeMn1Ni1.8 alloy from fragment of sleeve in centrifugal casting (**Stage 04c**)

sand casting

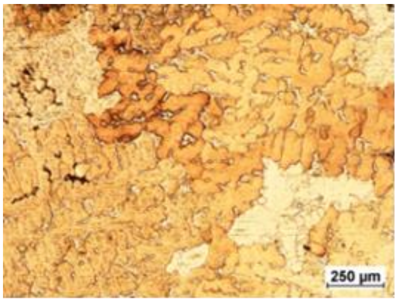

Fig. 8. Microstructure of CuSi3Zn3FeMn1Ni1 alloy in sand casting (**Stage 02s**)

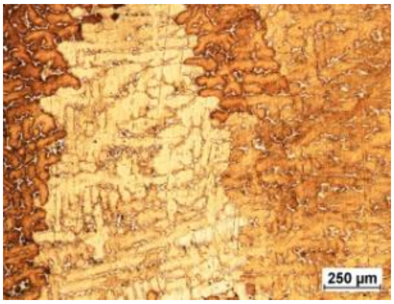

Fig. 9. Microstructure of CuSi3Zn3FeMn1Ni1.8 alloy in sand casting (**Stage 03s**)

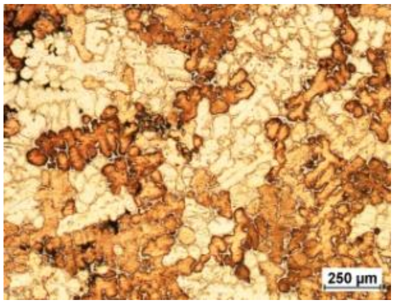

Fig. 10. Microstructure of CuSi3Zn3FeMn1Ni1.8+0.2Zr alloy in sand casting (**Stage 04s**)

gravity die casting

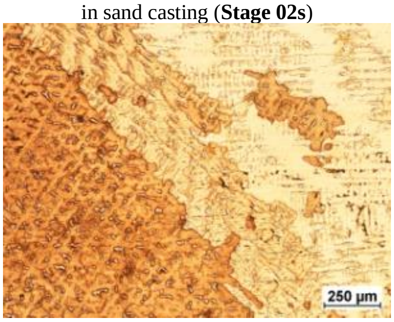

Fig. 11. Microstructure of CuSi3Zn3FeMn1Ni1 alloy of gravity die casting (**Stage 02d**)

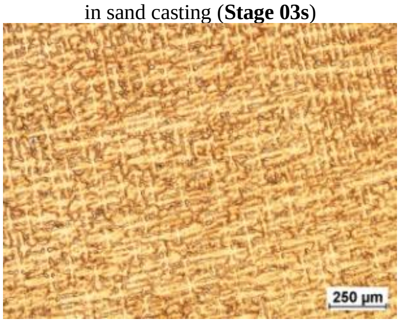

Fig. 12. Microstructure of CuSi3Zn3FeMn1Ni1.8 alloy of gravity die casting (**Stage 03d**)

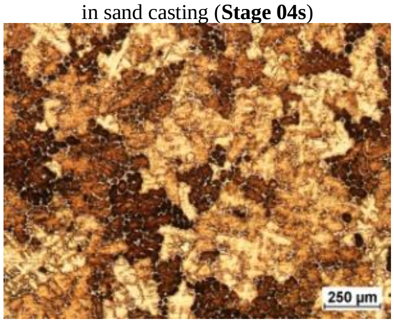

Fig. 13. Microstructure of CuSi3Zn3FeMn1Ni1.8+0.2Zr alloy of gravity die casting (**Stage 04d**)

The results of scanning electron microscopy (Figs. 14–17) indicated the presence of a mainly solid solution of Cu in the alloy along with the Zn, Si, and Fe elements. The analysis that was carried out confirmed the optical microscope observations. The nickel that was introduced into the alloy is visible at the grain boundaries; this formed an intermetallic compound together with silicon. The elemental distribution for the Stage 03s sample can be seen in the map (Fig. 14).

Tables 4–6 show the results of the microanalyses at the designated points. The phases that were present were consistent with the microscopic examination and the chemical composition of the tested alloy. The zirconium that was introduced into the alloy was visible as a component of one of the phases as well as undissolved precipitates (Figs. 15,17). On the other hand, the lead at a level of 0.27% in Alloy 04 was visible as an undissolved component (Figs. 16–17).

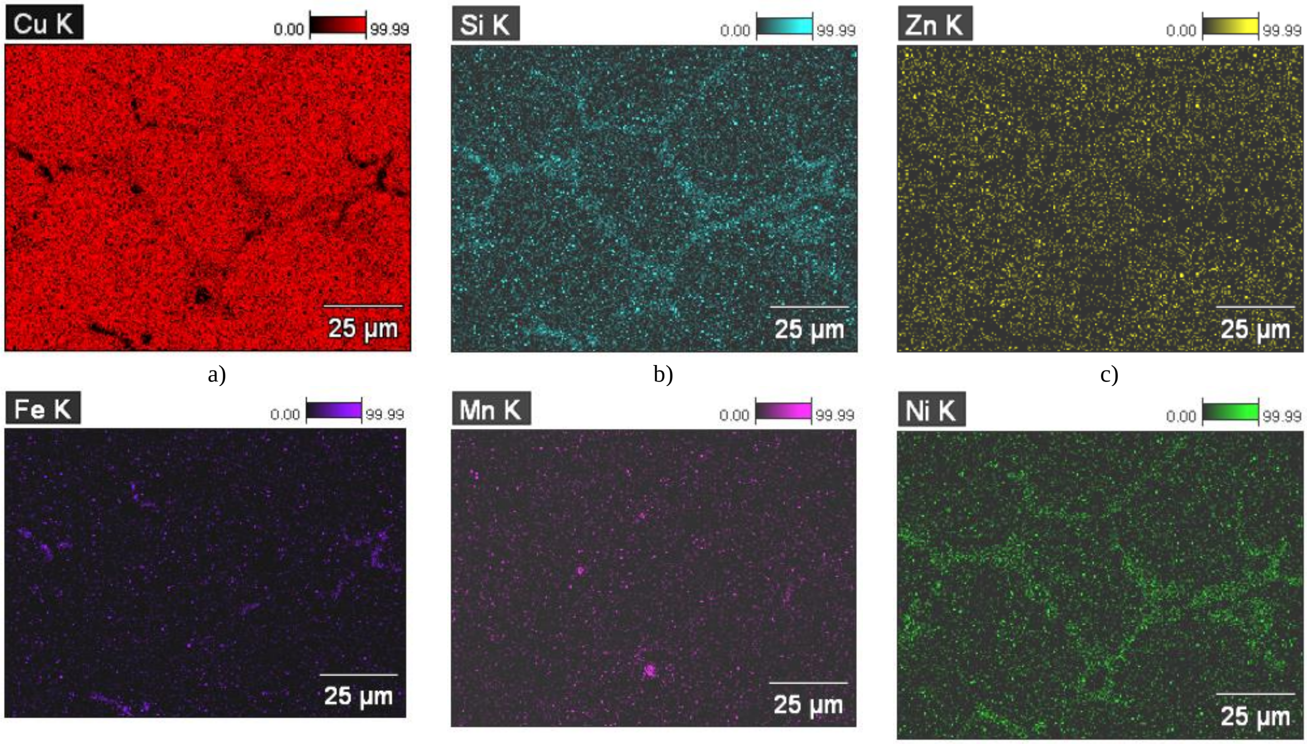

a) b) c)

d) e) f)

Fig. 14. Microstructures of CuSi3Zn3FeMn1Ni1.8 alloys in sand casting (**Stage 03 s**) – distribution of elements from EDS analysis: a) Cu; b) Si; c) Zn; d) Fe; e) Mn; f) Ni

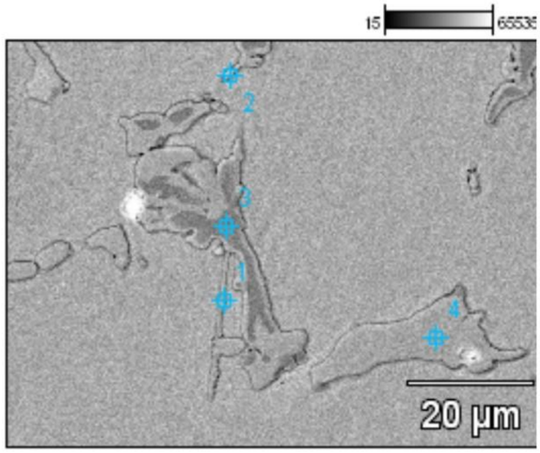

Fig. 15. SEM-EDS CuSi3Zn3FeMn1Ni1.8+0.2Zr alloy in sand casting (**Stage 04s**)

Table 4.
Results of microanalyses in microareas of Fig. 15

	Concentration (wt.%)						
pt	**Si**	**Mn**	**Fe**	**Ni**	**Cu**	**Zn**	**Zr**
04s pt1	10.37	1.88	10.53	12.39	55.23	-	9.61
04s pt2	7.67	1.13	0.83	8.05	80.28	2.05	-
04s pt3	17.89	3.32	42.16	27.35	7.14	-	2.13
04s pt4	8.64	1.15	0.98	13.84	75.38	-	-

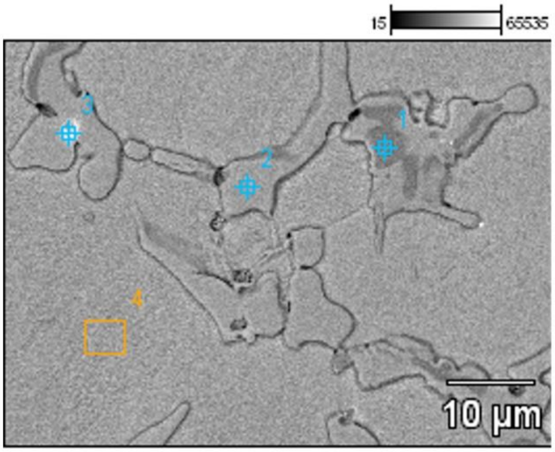

Fig. 16. SEM-EDS CuSi3Zn3FeMn1Ni1.8+0.2Zr alloy of gravity die casting (**Stage 04d**)

Table 5.
Results of microanalyses in microareas of Fig. 16

	Concentration (wt.%)						
pt	**Si**	**Mn**	**Fe**	**Ni**	**Cu**	**Zn**	**Pb**
04d pt1	19.20	5.48	43.07	23.56	8.68	-	-
04d pt2	8.86	1.08	1.39	13.11	75.56	0.89	-
04d pt3	1.86	-	0.59	3.20	21.71	-	72.16
04d pt4	2.60	0.58	0.67	1.73	88.87	5.55	-

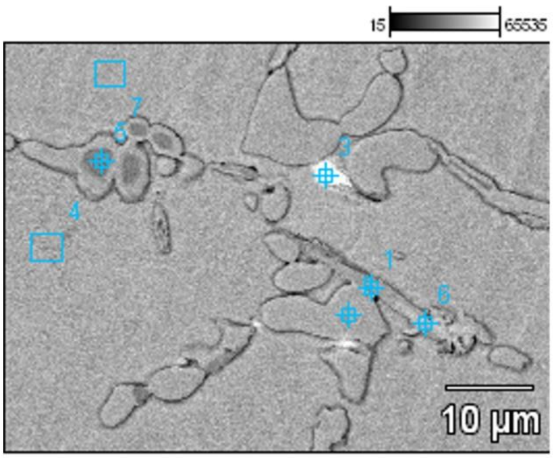

Fig. 17. SEM-EDS CuSi3Zn3FeMn1Ni1.8+0.2Zr alloy from fragment of sleeve in centrifugal casting (**Stage 04c**)

Table 6.
Results of microanalyses in microareas of Fig. 17

	Concentration (wt.%)							
pt	**Si**	**Mn**	**Fe**	**Ni**	**Cu**	**Zn**	**Zr**	**Pb**
04c pt1	13.58	3.35	25.91	23.05	11.14	-	22.97	-
04c pt2	8.68	0.93	-	13.00	77.39	-	-	-
04c pt3	-	-	-	-	11.96	-	-	88.04
04c pt4	3.33	1.22	0.88	2.61	87.50	4.46	-	-
04c pt5	18.61	6.48	42.29	24.40	8.21	-	-	-
04c pt6	7.40	1.62	15.51	13.91	9.03	-	52.53	-
04c pt7	3.02	0.80	1.03	1.98	87.40	5.77	-	-

4. Influence of alloy additions and casting parameters on mechanical properties

To determine how the mechanical properties of the bronze under study were affected by the casting technology, the castings were made with three options: gravity casting in a moulding compound, gravity casting in a die, and centrifugal casting in a machine with a horizontal axis of rotation. The different heat-dissipation rates and crystallisation conditions affected the alloy's strength, and the alloying elements and modifiers affected the mechanical properties and microstructures of the cast alloys. In order to determine how the strength of the CuSi3Zn3Mn1 bronze was affected by increased nickel contents and different casting parameters, a number of tests were performed (the results of which are summarised in Table 7).

By analysing Table 7 and the graph that is plotted against it (Fig. 18), we can see how the nickel content and casting technology affected the strength properties. The highest UTS value from the castings that were made in the sand moulds could be found in the primary sample (Stage 01s). The addition of 0.9% nickel caused a decrease in the yield strength and tensile strength as well as the elongation of the sample. We can see that both samples were made within the standard; the concentrations of the alloying elements significantly affected the strength parameters of the samples. When making castings according to the cited standard, it is reasonable to keep the nickel content low. Each of the mechanical parameters that were tested in the Stage 02 sample was lower than in the Stage 01 sample. Increasing the nickel content to 1.8% in Stage 03s resulted in significantly better mechanical properties than could be found in Stage 02s; however, the increased Ni content only benefited the hardness of the alloy in the GS technology. Due to the high melting point of nickel, the Stage 02s melt may have contained a higher amount of unmelted nickel metal than could be found Sample 03 (which had higher strength properties).

Table 7.
Results of mechanical property testing

Experiment	UTS [MPa]	Proof Stress [MPa]	A_{10} [%]	BHN
Stage 01s sand casting CuSi3Zn3Mn1	338.0	194.5	17.2	113
Stage 02s sand casting CuSi3Zn3Mn1+0.9%Ni	261.9	125.1	9.0	110
Stage 03s sand casting CuSi3Zn3Mn1+1.8%Ni	312.6	140.4	9.65	144
Stage 04s sand casting CuSi3Zn3Mn1 +1.8%Ni+0.2%Zr	297.6	107.9	8.65	117
Stage 01d die casting CuSi3Zn3Mn1	355.8	153.7	29.5	135
Stage 02d die casting CuSi3Zn3Mn1+0.9%Ni	361.7	178.0	24.0	105
Stage 03d die casting CuSi3Zn3Mn11+1.8%Ni	365.6	150.8	14.5	123
Stage 04d die casting CuSi3Zn3Mn1+1.8%Ni+0.2%Zr	341.2	179.5	11.5	137
Stage 04 die casting CuSi3Zn3Mn1+1.8%Ni+0.2%Zr (sleeve)	403.2	145.0	22.0	136

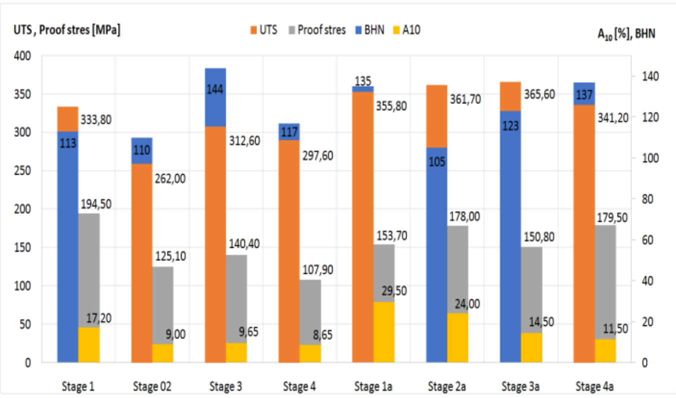

Fig. 18. Mechanical properties – graph

The samples that were taken from the die castings had significantly higher mechanical parameters than the samples that were cast into the moulding compounds. In the cases of the samples from the die castings, no significant effect of the nickel and zirconium could be seen on the mechanical properties of the alloy. In the sample in which the Ni content was 1.8%, the elongation decreased (Stages 03d and 04d).

In terms of the mechanical properties centrifugal technology proved to be the most favourable option.

5. Conclusions

The purpose of the study was to determine how the mechanical properties and microstructure of CuSi3Zn3Mn1 bronze were affected by the casting technology and the contents of certain alloying additives. Based on the results, it can be concluded that the mechanical properties and microstructures of the studied alloy were dependent on both factors.

- microstructure of studied alloy contained solid solution of copper and intermetallic phases;
- microstructure of metal poured into metal mould was finer than that which was cast into moulding compound;
- mechanical properties of castings made in moulding compound were lower than those that were cast into metal moulds;
- increased nickel content in tested bronze did not significantly affect its properties, BHN parameter improved;
- on basis of metallographic studies, occurrence of nickel at grain boundaries could be observed – this formed intermetallic compounds;
- zirconium introduced into alloy did not completely dissolve – its undissolved particles were visible.

Acknowledgements

The financial support of the State Committee for Scientific Research of Poland under the grant numbers 16.16170.7998 is acknowledged.

References

[1] Nnakwo, K.C., Mbah, C.N. & Nnuka, E.E. (2019). Influence of trace additions of titanium on grain characteristics, conductivity and mechanical properties of copper-silicon-titanium alloys. *Heliyon*. 5(10), e02471, 1-7. DOI: 10.1016/j.heliyon.2019.e02471.

[2] Rzadkosz, S., Kranc, M., Garbacz-Klempka, A., Kozana, J. & Piękoś, M. (2015). Refining processes in the copper casting technology. *Metalurgija*. 54(1), 259-262.

[3] Wesołowski, K. (1966). *Metaloznawstwo*. tom III. Warszawa: Państwowe Wydawnictwo Techniczne. (in Polish).

[4] Prowans, S. (1988). *Metaloznawstwo*. Warszawa: Państwowe Wydawnictwo Naukowe. (in Polish).

[5] Goto, I., Aso, S., Ohguchi, Ki., Kurosawa, K., Suzuki, H., Hayashi, H. & Shionoya, J. (2019). Deformation behavior of pure copper castings with as-cast surfaces for electrical parts. *Journal of Materials Engineering and Performance*. 28, 3835-3843. DOI: 10.1007/s11665-019-3865-5.

[6] Bydałek, A.W. & Najman, K. (2006). The reduction melting conduction of Cu-Si slloys. *Archives of Foundry*. 6(22), 107-110. (in Polish).

[7] Davis, J.R. (Ed.) (2001). Copper and copper alloys. ASM International.

[8] Rowley, M.T. (1984). *Casting copper-base alloys*. Illinois: American Foundrymen´s Society.

[9] Rzadkosz, S. (2013). *Foundry of copper and copper alloys*. Kraków: Akapit. (in Polish).

[10] Garbacz-Klempka, A., Kozana, J., Piękoś, M., Papaj, P., Papaj, M. & Perek-Nowak, M. (2018). Influence of modification in centrifugal casting on microstructure and mechanical properties of silicon bronzes. *Archives of Foundry Engineering*. 3(18), 11-18. DOI: 10.24425/123594.

[11] Romankiewicz, R., Romankiewicz, F. (2016). Research into oxide inclusions in silicon bronze CuSi3Zn3MnFe with the use of X-ray microanalysis. *Metallurgy and Foundry Engineering*. 42(1), 41-46. DOI: 10.7494/mafe.2016.42.1.41
[12] Tokarski, M. (1985). *Metaloznawstwo metali i stopów nieżelaznych w zarysie*. Katowice: Wydawnictwo Śląsk.
[13] Kosowski, A. (1996) *Metaloznawstwo stopów odlewniczych.* Kraków: Wydawnictwo AGH.
[14] Nnakwo, K.C., Osakwe, F.O., Ugwuanyi, B.C., Oghenekowho, P.A., Okeke, I.U. & Maduka, E.A. (2021) Grain characteristics, electrical conductivity, and hardness of Zn-doped Cu–3Si alloys system. *SN Applied Sciences*. 3(11), 829, 1-10. DOI: 10.1007/s42452-021-04784-1.
[15] Adamski, Cz. (1953). *Casting bronzes and silicon brasses - technology and application.* Warszawa: Państwowe Wydawnictwo Techniczne. (in Polish).
[16] Guharaja, S., Noorul Haq, A. & Karuppannan, K. M. (2006). Optimization of green sand casting process parameters by using Taguchi's method. *The International Journal of Advanced Manufacturing Technology*. 30, 1040-1048. DOI:10.1007/s00170-005-0146-2.
[17] Hirigo, T.H. & Singh, B. (2019). Design and analysis of sand casting process of mill roller. *The International Journal of Advanced Manufacturing Technology*. 105, 2183-2214. DOI: 10.1007/s00170-019-04270-4.
[18] Sadarang, J., Nayak, R.K. & Panigrahi, I. (2021). Challenges and Future Prospective of Alternative Materials to Silica Sand for Green Sand Mould Casting: A Review. *Transactions of the Indian Institute of Metals*. 74, 2939-2952. DOI: 10.1007/s12666-021-02370-y.
[19] Shamasundar, S. & Gopalakrishna V. (2004). *Gravity die casting. process die design and process optimisation*. esi-group, retrieved July 3, 2023 from https://www.esi-group.com/resources/gravity-die-casting-process-die-design-and-process-optimisation.
[20] Halvaee, A. & Talebi, A. (2001). Effect of process variables on microstructure and segregation in centrifugal casting of C92200 alloy. *Journal of Materials Processing Technology*. 118(1-3), 122-126. DOI: 10.1016/S0924-0136(01)00904-9.
[21] Malhotra, V. & Kumar Y. (2016). Study of process parameters of gravity die casting defects. *International Journal of Mechanical Engineering and Technology (IJMET)*. 7(2), March-April, 208-211.
[22] Balout, B. & Litwin, J. (2012). Mathematical modeling of particle segregation during centrifugal casting of metal matrix composites. *Journal of Materials Engineering and Performance*. 21, 450.462. DOI: 10.1007/s11665-011-9873-8.
[23] Wang, X., Chen, R., Wang, Q., Wang, S., Li, Y., Su, Y., Xia, Y., Zhou, G., Li, G. & Qu, Y. (2022). Influence of casting temperature and mold preheating temperature on centrifugal casting by numerical simulation. *Journal of Materials Engineering and Performance.* 32(15), 6786-3809. https://doi.org/10.1007/s11665-022-07608-4.
[24] Predein, V.V., Zhilin, S.G. & Komarov, O.N. (2022). Promising methods for forming the structure and properties of metal obtained by crystallization under the action of centrifugal forces. *Metallurgist.* 65(11-12), 1311-1323. https://doi.org/10.1007/s11015-022-01277-3.
[25] Sen, S., Muralidhara B.K. & Mukunda, P.G. (2020). Study of flow behaviour in vertical centrifugal casting. *Materials Today: Proceedings*. 24(2), 1392-1399. DOI: 10.1016/j.matpr.2020.04.457.
[26] Keerthi Prasad, K.S., Murali, M.S. & Mukunda, P.G. (2010). Analysis of fluid flow in centrifugal casting. *Frontiers of Materials Science in China*. 4, 103-110. DOI: 10.1007/s11706-010-0005-4.
[27] Wang, X., Chen, R., Wang, Q., Wang S., Li, Y., Xia, Y., Zhou, G., Li, G. & Qu, Y. (2023). Influence of rotation speed and filling time on centrifugal casting through numerical simulation. *International Journal of Metalcasting*. 17(2), 1326-1339. DOI: 10.1007/s40962-022-00841-6.
[28] Wołczyński, W., Ivanova, A. A. & Kwapisiński, P. (2019). On consonance between a mathematical method for the CET prediction and constrained / unconstrained solidification. *Procedia Manufacturing*. 30, 459-466. DOI: 10.1016/j.promfg.2019.02.065.
[29] Kwapisiński, P. & Wołczyński, W. (2023). Control of the CET localization in continuously cast copper and copper alloys' ingots. *Archives of Foundry Engineering*. 23(2), 91-99. DOI: 10.24425/afe.2023.144303.
[30] Wołczyński, W., Lipnicki, Z., Bydałek, A.W. & Ivanova, A. (2016). Structural zones in large static ingot. forecasts for continuously cast brass ingot. *Archives of Foundry Engineering*. 16(3), 141-146. DOI: 10.1515/afe-2016-0067.